# Characterization of Imprinted Microbeads Synthesized via Minisuspension Polymerization

Juan J. Torres, Hernán A. Montejano, Carlos A. Chesta*

The properties of MIPs synthesized by minisuspension polymerization are studied. The template is cyclododecyl 2,4-dihydroxybenzoate (**1**), which behaves as good mimic of the estrogenic mycotoxin zearalenone. 2-DAEM and EGDMA are used as functional and crosslinker monomers, respectively. The synthesized particles are characterized by optical and electronic microscopy, $N_2$ sorption measurements, and FT-IR spectroscopy. The molecular recognition capability of MIPs is evaluated by comparing the adsorption Freundlich isotherms of MIPs to those of the corresponding non-imprinted polymers. It is concluded that MSP is an attractive alternative for molecular imprinting because it is easy to apply and produces high yield of spherical particles of "tunable" size with acceptable molecular recognition capabilities.

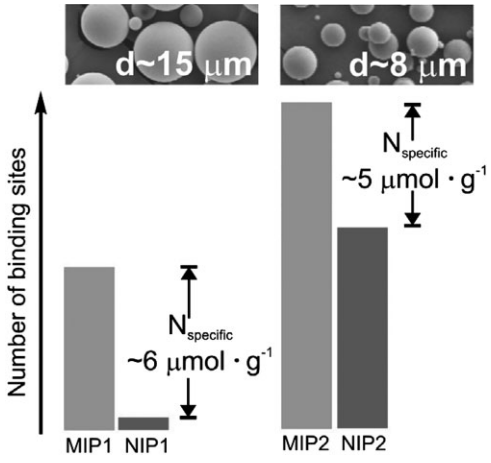


## 1. Introduction

The molecular imprinting of polymers is a technique that allows generating recognition sites in a polymer matrix for (almost) any compound of analytical interest by using the same compound as a template.[1] In the last decades, molecularly imprinted polymers (MIPs) have found a wide range of analytical and technological applications.[2–7]

MIPs are generally prepared by the conventional bulk polymerization method, which requires crushing and sieving.[8] This procedure is not only tedious, but also results in only moderated yields of (irregularly shaped) MIP particles of a wide size distribution. For some applications, for instance when MIPs are intended to be used as stationary phases in high-performance liquid chromatography (HPLC), this can be a serious disadvantage. For that reason, different synthetic strategies such as precipitation,[9] miniemulsion,[10] multi-steps swelling,[11] suspension,[12–18] etc., have been implemented to control the morphology of the MIP particles and thus to improve their chromatographic performances.

Among these alternative imprinting methods, suspension polymerization (SP) is a very attractive technique due to its easy applicability and high yields of regular (spherical) particles. Basically, SP is a technique in which water-insoluble monomers, small amounts of a stabilizer such as poly(vinyl alcohol) (PVA) and high stirring rates are used. In the conventional SP method, emulsion of the monomer is achieved by using standard impellers ($\leq$2 000 rpm), while minisuspension polymerization (MSP) requires much higher stirring rates ($\approx$10 000 rpm).[19–21] It is well established that the (average) size of the obtained polymeric particles strongly depends on the stirring rate used during the polymerization process. In spite of the advantages of the SP and MSP techniques they show also several drawbacks, at least for some particular applications. For instance, the conventional SP technique is not suitable for the preparation of MIPs as HPLC stationary phases because large size particles (30–450 μm) are invariably obtained. These

J. J. Torres, H. A. Montejano, C. A. Chesta
Departamento de Química, Universidad Nacional de Río Cuarto, (5800) Río Cuarto, Argentina
E-mail: cchesta@exa.unrc.edu.ar


© 2012 WILEY-VCH Verlag GmbH & Co. KGaA, Weinheim

DOI: 10.1002/mame.201100237

particles have been successfully used however for solid-phase extractions (SPE).[16–18] An interesting aspect of the SP technique is that synthesis of smaller particles, such as those required HPLC applications (ca. 2–30 μm) and typically obtained by using the MSP method, can be achieved under mild stirring rates using a combination of stabilizers; e.g., PVA and sodium dodecyl-sulfate (SDS).[19,20] It was shown that SDS and PVA produced a remarkably enhancement on the minisuspension stability acting cooperatively. The electrostatic repulsion between several SDS molecules (a negatively charged surfactant) associated with PVA on the surface of the minidroplets, causes the stretching of the polyol chains and concurrently, creates vast charged areas on the surfaces of the droplets. These repulsive forces preclude the approach of the minidroplets and delay their coalescence. To the best of our knowledge, the only MIPs prepared by using this (modified) SP technique (strictly speaking, the MSP technique) were recently reported by Khan et al.[13,22]

Another disadvantage of the SP techniques for the synthesis of MIPs is related to the large (molar) excess of the dispersing phase-stabilizing agents (relative to the amount of functional monomers) required for obtaining the metastable prepolymerizable dispersions. In principle, it is expected the dispersing phase (water) and stabilizers (PVA or PVA/SDS) to interfere and reduce the number (and strength) of the interactions between the functional monomers and the template. This should result in poor performances of these microbeads for molecular recognition, particularly if the interactions between the functional monomer and the template are mainly of the H-bonding type. The use of non-aqueous dispersant phases has been proposed (and successfully tested) to avoid these effects.[17,18,23] However, after a thorough review of the MIP literature, we were able to find only vague references to failed attempts to prepare MIPs by the conventional MSP technique; failures that in principle could be ascribed to the interferences of the water/stabilizer (molar excess) during the imprinting process.[9,24,25] Furthermore, the successful imprinting reported by Khan et al.[22] using the (modified) SP method suggests that these interferences are apparently not as important as it was anticipated. These facts encouraged us to further investigate the synthesis of microbeads using the modified SP method, putting special emphasis on the analysis on the type (and strength) of the interactions established between the template and the polymers.

We report herein a study on the properties of two MIPs synthesized by a (modified) MSP technique and a MIP synthesized in bulk. The template chosen for this study was cyclododecyl 2,4-dihydroxybenzoate (**1**, Scheme 1), a compound that was successfully used by Urraca et al.[26] as a mimic of the estrogenic mycotoxin zearalenone

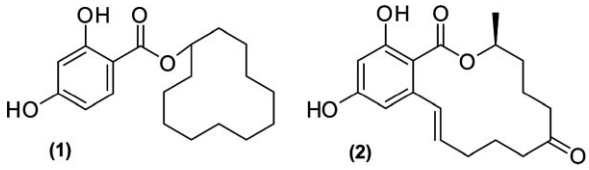


*Scheme 1.* Structures of the emulator (**1**) and the zearalenone (**2**).

(**2,** Scheme 1). We choose (**1**) as template because it is practically insoluble in water and given its structure, the synthesized MIPs could be of significant interest in food and environmental chemistry. The functional and crosslinker monomers used were 2-(diethylamino)-ethyl methacrylate (2-DAEM) and ethylene glycol dimethacrylate (EGDMA), respectively. The synthesized polymeric particles were characterized by optical and electronic microscopy, $N_2$ sorption measurements, and Fourier-transform infrared (FT-IR) spectroscopy. The molecular recognition behavior of the MIPs was examined by analysis of the affinity and specificity of the polymers, data obtained from typical HPLC elution and frontal analysis experiments.

## 2. Experimental Section

### 2.1. Materials

2-DAEM (99%), EGDMA (98%), PVA (Mowiol 6-98, $\overline{M}_w \approx 47\,000$; 98.0–98.8 mol hydrolysis), SDS (98%), 1,1′-carbonyldiimidazole (≥97%), 2,4-dihydroxybenzoic acid (≥98.0%), cyclododecanol (99%), 1,8-diazabicyclo[5.4.0]undec-7-ene (98%), and potassium bromide were purchase from Sigma-Aldrich (Argentina). 1,1′-Azobis(cyclohexane-1-carbonitrile) (V-40) was supplied by Wako Chemicals (USA). PVA and SDS were used as received. 2-DAEM and EGDMA were purified through a column filled with De-Hibit-200 (Polysciences) which specifically retains the stabilizer. All solvents used were of analytical or HPLC grade.

(**1**) was synthesized from 2,4-dihydroxybenzoic acid and cyclododecanol following the procedure published by Urraca et al.[26] The purification of (**1**) was carried-out by column chromatography, using silica gel (Analtech, particle size 35–75 μm) as stationary phase and a mixture of cyclohexane and ethyl acetate (3:2 v/v) as eluent. The structure of (**1**) was corroborated by mass spectra, $^{13}C$ and $^{1}H$ NMR, UV-Vis and fluorescence spectroscopy. $^{1}H$ NMR ($CDCl_3$, $\delta$): 1.36 (s, 2-H), 1.67 (s, 2H), 3.88 (m, 1H), 6.26 (d, 1H), 6.30 (dd, 1H), 7.74 (d, 1H), 11.14 (s, 2H). $^{13}C$ NMR ($CDCl_3$, $\delta$): 20.9, 20.1, 23.1, 23.2, 23.3, 23.8, 23.9, 24.1, 29.0, 32.2, 73.4, 103.0, 106.2, 107.7, 131.8, 162.0, 163.5, 169.7. MS (70 eV): $m/z = 320$ (2) ($M^+$), 166 (10), 154 (100), 137 (64), 136 (95), 135 (35), 109 (15), 81 (37). UV (MeCN): $\lambda_{abs}^{max}$ ($\varepsilon$): 257 nm (9 900 $L \cdot mol^{-1} \cdot cm^{-1}$), 297 nm (4 400 $L \cdot molmol^{-1} \cdot cm^{-1}$). Fluorescence (MeCN): $\lambda_{em}^{max} = 315$, 425 nm. Solubility tests indicate that (**1**) is insoluble in water but substantially soluble in organic (protic and non-protic) solvents.


© 2012 WILEY-VCH Verlag GmbH & Co. KGaA, Weinheim

### 2.2. Instruments

Absorption spectra were recorded with a Hewlett-Packard diode array spectrophotometer 8452.

The fluorescence spectra were obtained with a Spex fluorometer (Fluoromax) equipped with software DM 3000 3.2.

FT-IR spectra were recorded using a FT-IR Nicolet Impact 400.

$^1$H NMR spectra were recorded in a Bruker 200 (200 MHz). The mass spectrum of (**1**) was obtained using a Hewlett Packard 5890 GC-mass chromatograph equipped with an HP-5 (5% PH-ME silicone) column (30 m × 0.32 mm × 0.25 μm). HPLC chromatographic studies were performed using a Waters 1525 binary HPLC chromatograph equipped with a Varian 2550 absorbance detector.

Polymerizations were carried-out in a Rayonet photoreactor fitted with 2, 4, or 6 F8T5/BLB Philips UV lamps ($\lambda = 350$ nm, 8 W each) depending upon the experiment. The SPs were carried out in a cylindrical homemade round-bottom glass reactor (250 mL) equipped with four deflectors and an impeller with two vertical flat plates. The geometric dimensionless numbers that characterize the reactor are: $S_1 = 0.33$; $S_2 = 1$; $S_3 = 0.25$; $S_4 = 0.25$; $S_5 = 0.1$; $S_6 = 1$.[27,28] The suspension was continuously stirred using a rod stirrer (Glas-Col dual-axis maximum RPM: 333/4 000) with variable speed control.

The imprinted and non-imprinted polymers (MIPs and NIPS, respectively) obtained from bulk polymerization were ground manually and sieved to select particles between 25 and 53 μm. Zonytest sieves ASTM 270 (53 μm) and ASTM 500 (25 μm) were used for this purpose.

The packing of the analytical columns was done with an Eldex laboratories pump mod. AA-100-5-2 eluting at flow rate of 4.5 mL · min$^{-1}$.

Photoimages of the droplets and particles synthesized were obtained with an Arcane XSZ-107E microscope equipped with a digital camera Moticam 1000. The sizes of the particles were evaluated using the software Motic Images Plus 2.0 ML image.

Micrographs were obtained using a variable pressure LEO 1450VP SEM working at 15 kV. To this end, polymer beads were placed on aluminum pegs and sputter coated with 15 nm of gold using a SPI sputter coater.

Average pore diameter and surface area of the particles was obtained using a BET Micromeritics Series 680, Accusorb 2100E-210-00001-01.

### 2.3. Synthesis of Spherical Beads via the Modified SP Technique: MIP1, NIP1, MIP2, and NIP2

Syntheses of MIPs (MIP1, MIP2) were carried-out following the method described by Khan et al.[22] although the amounts of PVA and SDS and the stirring rates used for the synthesis were choose from a series of optimization size particles experiments (see Results and Discussion section). Initially, a mixture consisting of: (**1**) (1 mmol, 320 mg), 2-DAEM (4 mmol, 741 mg), EGDMA (20 mmol, 3 960 mg), toluene (5 mL), V-40 (0.91 mmol, 222 mg), and PVA (3 g, dissolved in 150 mL of water) were placed in the cylindrical reactor. The mixture was stirred at constant speed (1 616 and 2 150 rpm for MIP1 and MIP2, respectively) for 30 min. During this lapse, the sample was deoxygenated by bubbling nitrogen. Finally, SDS (1.73 mmol, 500 mg) dissolved in 20 mL of water was added to the reactor. The mixture was continued stirring at constant speed for 1 h at room temperature, always under $N_2$ atmosphere. The NIPs (NIP1, NIP2) were prepared in the same way but without adding (**1**). The polymerizations were initiated photochemically, at room temperature, with four UV lamps illuminating at 350 nm for 2 h. The obtained polymers beads were filtered (Whatmann 3) and dried overnight at 50 °C at reduced pressure (30 torr). The polymers were finally cleaned as describe in the section of particle's packing. The yields of the (cleaned) polymers were in all the cases >80%. The average diameters (and corresponding standard deviations) were calculated by analysis of ten photographs obtained in a microscope equipped with a digital camera. As expected, the particle diameters of MIP1 (and NIP1) are larger than those obtained for MIP2 (and NIP2). FT-IR spectra of the dried polymers were obtained dispersing ≈1 mg of the polymers in 500 mg of KBr (≈0.2 wt%).

### 2.4. Synthesis of the Irregular Beads, Bulk Polymerization: MIP3, NIP3, MIP4, and NIP4

MIP3 was synthesized from a mixture containing: (**1**) (1.3 mmol, 417 mg) in 13 mL of acetonitrile, 2-DAEM (5.2 mmol, 963 mg), EGDMA (26 mmol, 5 154 mg), and V-40 (0.611 mmol, 149 mg). The mixture was purged with $N_2$ for 30 min in sealed tubes. The polymerization was initiated photochemically with four UV lamps ($\lambda = 350$ nm). The irradiation of the samples was kept for 6 h at room temperature. The NIP3 was performed in the same way but without adding (**1**). The polymers were finely ground in a mortar and dried at 50 °C under reduced pressure (30 torr). Finally the particles of size between 25–53 μm were selected by using sieves. The polymers were cleaned as describe in the section of particle's packing. The yields of (cleaned) particles of suitable size were always ≈30%. MIP4, NIP4 were synthesized in the same way but using toluene as the porogen solvent. FT-IR spectra of the dried polymers were obtained dispersing ≈1 mg of the polymers in 500 mg of KBr (≈0.2 wt%).

### 2.5. Packing of the Polymeric Particles in the HPLC Columns

The polymeric particles were suspended in methanol (13 wt%) and sonicated for 10 min. Particles packing was carried out using two empty commercial stainless steel HPLC columns (Hichrom, UK); one of 4.6 mm id × 250 mm (used as reservoir) and a second column of 4.6 mm id × 150 mm. The last column was used for the chromatographic studies (working column). The columns were connected in series by a plug adapter and sealed by a frit outlet. The column system was placed vertically and the slurry added to fill ≈ $^3/_4$ of the reservoir column. The system was connected to an Eldex laboratories pump and eluted with water at a rate of 4.5 mL · min$^{-1}$. Typically, the volume of water used in the washing process of the polymers was equivalent to 100 times the column system (≈7 mL). The cleaning procedure was completed eluting the column with 200 mL of methanol. The choice of water and methanol as mobile phases should warranty the elimination of SDS, PVA, (**1**) and other unwanted polymerizations byproducts initially present in the polymeric matrices. Finally, the reservoir column was detached and a frit was placed on top of the working column. This procedure


© 2012 WILEY-VCH Verlag GmbH & Co. KGaA, Weinheim

worked well for packing all polymers excepting MIP4 and NIP4. Apparently, these two polymers are mechanically fragile (or compressible) and collapse during packing as confirmed by the rapid increase of the system backpressure observed (>4 500 psi) and consequently they were discarded for the HPLC studies. It is somehow strange that the MIP synthesized with toluene did not work, particularly when other researchers have published the used of similar polymers as stationary HPLC phases.[12,29] Packing of the HPLC columns with irregular particles is generally difficult due to the presence of particles smaller than 25 μm.[30] These small irregular particles seem to pack densely carrying the pressure of the system to values of non-operability. Hence, before packing, the sub-μm particles were removed by suspending the polymer in methanol, allowing the decantation of larger particles and removing the supernatant. This procedure was repeated at least four times until acceptable pressures during packing were obtained.

The masses of polymers packed in the columns were of 0.64, 0.84, 0.46, 0.61, 1.10, 0.47 g for MIP1, MIP2, MIP3, NIP1, NIP2, NIP3, respectively. Apparently, the reduction in the size and the improvement of the regularity of the particles significantly increases the efficiency of the packaging, as it can be concluded from the relative amounts of the materials incorporated into the column.

### 2.6. Chromatographic Evaluation of the MIPs

#### 2.6.1. Elution Chromatography

Columns filled with the different polymers were equilibrated with acetonitrile until reaching a constant UV reference signal. All experiments were performed at 1 mL · min$^{-1}$ of the mobile phase and the analytes [acetone and (**1**)] detected simultaneously by setting the UV detector at 257 nm. All experiments were carried out at room temperature, injecting into the columns 20 μL of a solution of (**1**) $3 \times 10^{-4}$ M. Acetone was used as dead volume marker. The retention factors ($k$) were calculated according to $k = (t - t_0)/t_0$, where $t$ is the analyte retention time and $t_0$ is the retention time of the acetone. The imprinting factors (IF) were calculated according to IF $= k_{MIP}/k_{NIP}$, where $k_{MIP}$ and $k_{NIP}$ represent the retention factor measured for the MIP and NIP, respectively. The reported uncertainties correspond to the average of three independent measurements of IF. The main source of errors arises from the measurement of the retention times of the acetone ($t_r^{vm}$). Small variations in $t_r^{vm}$, say ± 5 s, introduces large variations in the calculated IF.

#### 2.6.2. Frontal Chromatography

The binding properties and the MIP site's heterogeneity were evaluated from typical frontal analysis experiments.[31,32] The same columns were used for the frontal analysis and elution experiments. The two pumps of the solvent delivery system were used to obtain the breakthrough curves. One of the pumps delivered the pure acetonitrile as mobile phase, the other pump delivered a solution of the (**1**) $2 \times 10^{-3}$ M prepared in the same solvent. The concentration of the studied compound in the steady stream (from $1 \times 10^{-6}$ to $2 \times 10^{-3}$ M) was determined by the concentration of the sample solution and the flow-rate fractions delivered by the two pumps at constant flow rate (1 mL · min$^{-1}$) for a set time interval. At each concentration of (**1**), the breakthrough curve was recorded by allowing a sufficiently long delay time (90–120 min) between each successive curve to allow the re-equilibrium of the column with the pure mobile phase. The plateaux reached after the sorption experiments were recorded for more than 10 min before starting the determination of desorption's breakthrough curves. All experiments were carried-out setting the UV detector at 257 nm. The amount of (**1**) adsorbed ($B$) in each experiment expressed as μmol · g$^{-1}$ (μmol per g of MIP) were calculated by integration of the areas of desorption breakthrough curves.[31,32] The adsorption isotherms were constructed by plotting the experimental $B$ as a function of the concentration of (**1**) in the mobile phase; i.e., $F(M)$. The isotherms were analyzed using the Freundlich model.[33]

### 2.7. Nitrogen Sorption

Nitrogen sorption analysis was carried out on ≈40 mg of each polymer using a Gemini V2.0 surface area and pore size analyzer (Micrometrics). Twenty four point adsorption/desorption isotherms were generated and the surface area of the polymers was derived from the adsorption isotherm (in the range $P/P_0 < 0.3$ for a six point plot) using Brunauer, Emmett, and Teller (BET) analysis. Pore analysis was carried out using the Barrett, Joyner, and Halden (BJH) method.[34] Pore radii at each $P/P_0$ point was calculated using the Kelvin equation,[35,36] which was corrected for multilayer adsorption using the Halsey thickness equation.[37] Differential pore volumes were generated by plotting $dV/dD$ versus $D$, where V represents the pore volume and $D$ is the pore diameter.[37]

## 3. Results and Discussion

### 3.1. Synthesis of the Particles

Before the synthesis of the particles using the modified SP method, the characteristics of the microdroplets of the prepolymeric mixture were analyzed in order to choose the optimal conditions (composition of the mixture and stirring rates) of polymerization. This allowed setting the variables to obtain regular particles of the desired sizes.

At this point, it is worth to emphasize the importance of the design of the reactor in obtaining stable suspension at relatively low stirring rates. Indeed, the cylindrical reactor used in this study (see Experimental Section) proved to be much more effective than spherical reactors traditionally used for the synthesis of MIPs. Simple experiments performed using both type of reactors showed that to obtain microdroplets of the same (average) size, stirring rates up to four times higher were required for the spherical reactor. The advantages of cylindrical reactors (and the use of deflectors) to improve mixing efficiencies are well known


© 2012 WILEY-VCH Verlag GmbH & Co. KGaA, Weinheim

to chemical engineers. Bates et al. and Nienow and Miles[27,28] have discussed in detail the theoretical background related to the design of such type of reactors. Cylindrical reactors are easy to build and allow obtaining stable minisuspensions using standard impellers available in most labs in the world. Thus, in this study all syntheses were performed using the cylindrical reactor because this proved to be much more ductile to control the particle's size. Initially, 150, 2, 0.8, and 3.8 mL of water, toluene, 2-DAEM, and EGDMA, respectively, were mixed in the cylindrical reactor. To this mixture, 220 mg of the photoinitiator (V-40) and 417 mg of (**1**) were added. In total, ≈20 experiments were carried-out in which the stirring rate was varied between 760 and 2 200 rpm and the effect of adding different amounts of PVA and SDS studied. For each experiment, the droplets were photographed using an optical microscope equipped with a digital camera.

From these experiments some qualitative conclusions were reached. To this regard, a more detailed study is being conducted and it will be published elsewhere. For example, it was observed that a fixed concentration of PVA and stirring rate, the addition of SDS produced a decrease of the (average) size of the droplets accompanied by a remarkably decrease in their coalescence rate. On the other hand, keeping constant the amount of PVA and SDS dissolved and increasing the stirring rate, a progressive decrease the (average) size of the droplets was observed. From these experiments, two synthesis conditions were selected. In both syntheses, the same amounts of PVA and SDS were used (3 000 mg and 500 mg, respectively) at two different agitation rates: 1 620 (MIP1) and 2 200 rpm (MIP2). The calculated average diameters of the synthesized particles ($D_p$) and those of the corresponding prepolymeric droplets ($D_d$) are reported in Table 1. It should be noticed that an acceptable correlation between the size of the particles obtained and the size of the oil microdroplets of the prepolymeric mixture was observed in both cases. The widths of the particle size distribution ($\sigma_p$, $\sigma_d$), estimated as indicated in the Experimental Section, are reported in the same table.

*Table 1.* Diameters ($D_p$, $D_d$) and distribution ($\sigma_p$, $\sigma_d$) sizes of the droplets in the prepolymeric mixtures and particles synthesized using different methods and conditions.

| Polymer | $D_d$ [μm] | $\sigma_d$ [μm] | $D_p$ [μm] | $\sigma_p$ [μm] |
|---|---|---|---|---|
| NIP1 | 14 | 7 | 16 | 9 |
| MIP1 | 13 | 8 | 15 | 8 |
| NIP2 | 5 | 2 | 4 | 2 |
| MIP2 | 7 | 7 | 8 | 6 |
| NIP3 | – | – | 25–53 | – |
| MIP3 | – | – | 25–53 | – |

Figure 1 shows optical photograph of the microdroplets from the prepolymeric mixture of MIP2 (a) and the SEM micrographs obtained for MIP2 (b) and MIP3 (c) at a magnification 400 ×. The inserts in Figure 1(b, c) are the micrographs obtained at 6 000 ×. As shown, the

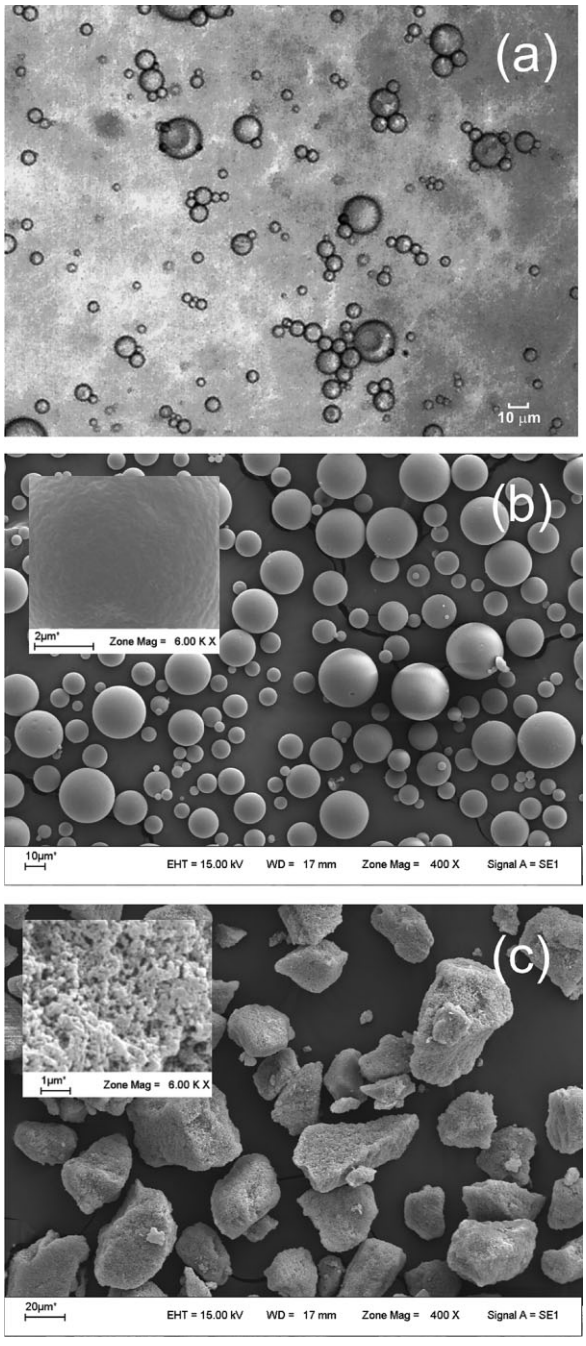


*Figure 1.* Optical photography of the microdroplets of the prepolymeric mixture of MIP2 (1a). SEM micrographs of MIPs made of poly(2-DAEM-*co*-EGDMA) prepared by the MSP (MIP2, 1b) and by the bulk polymerization method (MIP3, 1c). Magnification 400×. Inserts: surface detail obtained at a magnification 6 000×.


© 2012 WILEY-VCH Verlag GmbH & Co. KGaA, Weinheim

porosity on the particle surfaces seems to differ markedly. From Figure 1(b) can be concluded that the particle size distribution is broad, fact that is consistent with the above mentioned analysis of the optical images.

As a part of the characterization of the particles, FT-IR spectra for the different polymers were obtained. The spectrum of MIP3 shows strong absorptions at ≈2 900 (C−H), ≈1 725 (C=O) and several intense peaks between 1 500 and 600 $cm^{-1}$. The observed spectrum is quite similar to the reported for poly(EGDMA) and other related polymers.[38] The FT-IR spectra obtained for MIP1 and MIP2 after exhaustive washing (and drying) are shown in Figure 2. These spectra show certain peculiarities. First, the absorption due to the carbonyl groups (≈1 730 $cm^{-1}$) shows an important broadening, effect that is more pronounced for the smaller particles (MIP2). Both spectra also show a weak absorption at ≈3 400 $cm^{-1}$ and the peak at 2 900 (C−H) has a shoulder around 3 000 $cm^{-1}$. PVA (98 mol% hydrolysis) shows a weak absorption band near 3 400 and a more intense peak around 3 000 $cm^{-1}$, both due to the O−H stretching.[39] The polyalcohol also exhibits a series of intense peaks in the 1 500–650 $cm^{-1}$ spectral range. Thus, from the spectra in Figure 2, it cannot be concluded that all the PVA has been removed from the microspheres despite the thorough washing process. To the best of our knowledge, excepting those published by Khan and Park,[13] FT-IR spectra of particles obtained by the SP technique have not been reported in the literature. Unfortunately, the spectra published by Khan and Park[13] are not helpful in deciding whether significant amounts of PVA remain in the microbeads since the functional monomer used by these authors, ca. methacrylic acid, shows absorptions that strongly overlaps with the IR spectrum of the polyalcohol.

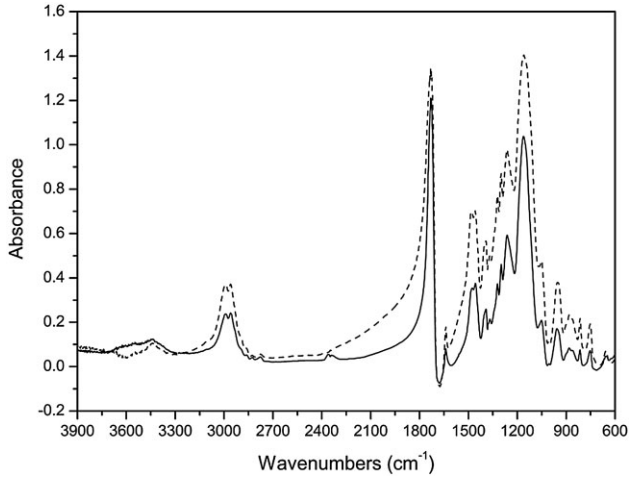


*Figure 2.* FT-IR spectra of MIP1 (solid line) and MIP2 microbeads (dashed line) (≈0.2 wt% in KBr).

### 3.2. Effects of Particle Morphology on the Retention and Imprinting Factors

Figure 3 shows the chromatograms of (**1**) on (a) MIP1/NIP1, (b) MIP2/NIP2, and (c) MIP3/NIP3 obtained using acetonitrile as mobile phase. The sharp fronting and peak tailing observed from the chromatogram obtained on MIP3 (c) is typical of stationary phases which present non-linear adsorption isotherms. The considerable peak broadening observed for MIP1 (a) and MIP2 (b) is likely to be caused by their particular large binding site's heterogeneity (vide infra) and slow mass transfer.[40,41] As usually observed,[29,41] the chromatograms obtained on the corresponding NIPs display better peak shapes.

Table 2 collects the retention ($k$) and IF factors calculated from the retention times measured for (**1**) ($t_r^{(1)}$) and acetone ($t_r^{vm}$). As shown, the estimated IF are only modest. However,

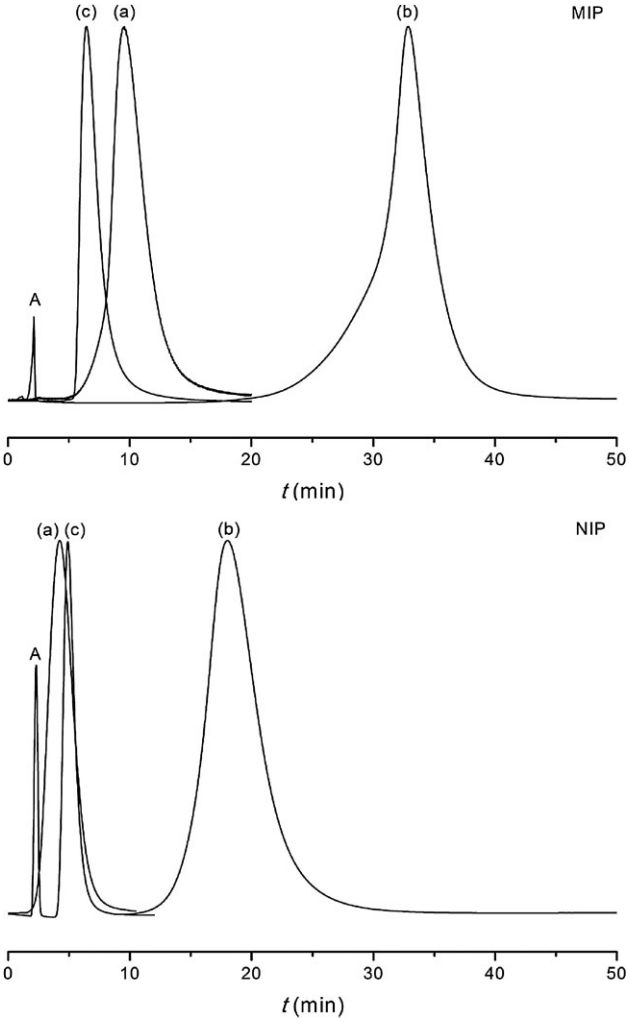


*Figure 3.* Chromatograms of (**1**) on (a) MIP1/NIP1, (b) MIP2/NIP2, and (c) MIP3/NIP3. HPLC conditions: column size, 150 mm × 4.6 mm id; temperature, 20 °C; mobile phase, acetonitrile; detection, 257 nm; flow rate, 1 mL · $min^{-1}$. Loaded amount of (**1**), 6 nmol.


© 2012 WILEY-VCH Verlag GmbH & Co. KGaA, Weinheim

*Table 2.* Retention times measured for (**1**) ($t_r^{(1)}$) and acetone ($t_r^{vm}$), capacity factors (*k*) and IF for the different polymers studied using acetonitrile as mobile phase. Loaded amount of (**1**), 6 nmol.

| Polymer | $t_r^{vm}$ [min] | $t_r^{(1)}$ [min] | *k* | IF |
|---|---|---|---|---|
| NIP1 | 2.2 | 4.2 | 0.9 | |
| MIP1 | 2.1 | 9.6 | 3.6 | $3.9 \pm 0.7$ |
| NIP2 | 1.8 | 17.9 | 8.9 | |
| MIP2 | 2.1 | 32.8 | 14.6 | $1.7 \pm 0.2$ |
| NIP3 | 2.3 | 4.9 | 1.1 | |
| MIP3 | 2.1 | 5.8 | 1.8 | $1.6 \pm 0.3$ |

it must be emphasized here that these IFs can be taken only as a corroboration of the imprinting process. MIPs (and NIPs) generally exhibit wide distributions of binding sites affinities and consequently, the observed $t_r^{(1)}$ vary with the amount of analyte injected into the column.[42,43] For instance, when 1.2, 6, and 40 nmol of (**1**) were injected in the column packed with MIP3, the residence times ($t_r^{(1)}$) change from 6.2, to 5.8 and 5.3 min, respectively. Although much less pronounced, the same effect is observed for the corresponding NIP. As a result, the calculated IF increases with decreasing amounts of (**1**) loaded. Thus, the $t_r^{(1)}$ (and IF) collected in Table 2 cannot be used to characterize (or even less to compare) the MIPs. As shown in the next section, conclusions about the recognition capabilities of the MIPs can only reached by comparing the corresponding binding isotherms.

### 3.3. Frontal Chromatography

Frontal chromatography experiments[31,32,44] were conducted to determine the adsorption-desorption isotherms of (**1**) on the MIPs and NIPs. Figure 4 shows the desorption breakthrough curves obtained for MIP3. The isotherms were constructed as indicated in the Experimental Section and fitted to the Freundlich isotherm model according to Equation 1 or 2:

$$B = aF^m \tag{1}$$

$$\log(B) = \log(a) + m\log(F) \tag{2}$$

In Equation 1, *a* and *m* are the fitting parameters of the Freundlich isotherm. *m* is the heterogeneity factor (or index) and it is related to the relative populations of high to low affinity sites in the polymer. Its value ranges from 0 to 1 and increases as heterogeneity decreases. Thus, small m indicates high heterogeneity of affinity binding

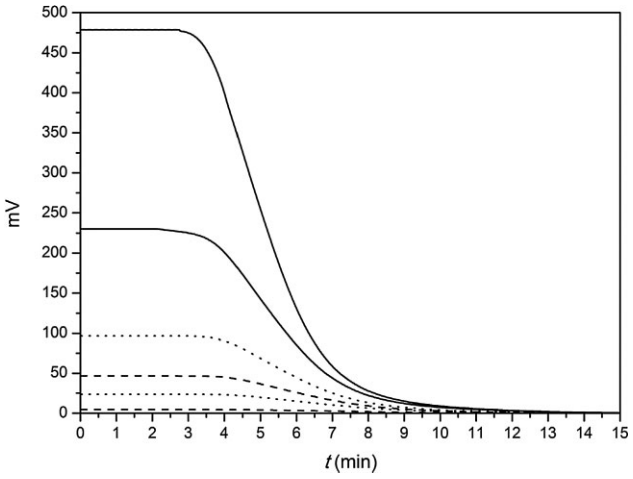


*Figure 4.* Desorption breakthrough curves obtained for MIP3.

sites in the material studied; while large m manifest the opposite phenomenon. The pre-exponential factor *a* is related to the binding affinity of the polymer. Rampey et al.[33,45] showed that the experimental parameters *m* and *a* can be used to estimate the affinity binding site's distribution: $N_i(K_i)$, the total number of binding sites (capacity): $N_{K_{min}-K_{max}}$ and the average affinity of the sites: $\overline{K}_{K_{min}-K_{max}}$, according to:

$$N_i(K_i) = 2.3am\left(1-m^2\right)K_i^{-m} \tag{3}$$

$$N_{K_{min}-K_{max}} = a\left(1-m^2\right)\left(K_{min}^{-m} - K_{max}^{-m}\right) \tag{4}$$

$$\overline{K}_{K_{min}-K_{max}} = \left(\frac{m}{m-1}\right)\frac{\left(K_{min}^{(1-m)} - K_{max}^{(1-m)}\right)}{\left(K_{min}^{-m} - K_{max}^{-m}\right)} \tag{5}$$

It is worth noting that the affinity distributions calculated from Equation 3 are only valid within a certain range of binding affinities: $K_{min} = 1/F_{max}$ and $K_{max} = 1/F_{min}$, which are defined by the concentration limits of the experimental binding isotherms ($F_{min}$ and $F_{max}$). Figure 5 shows the isotherms obtained for the series of MIPs and NIPs studied. As shown, the isotherms are acceptably fitted to the Freundlich model (Equation 2). Table 3 collects the experimental *a* and m and the weighted average affinity ($\overline{K}_{K_{min}-K_{max}}$) and the number of binding sites ($N_{K_{min}-K_{max}}$). The reported uncertainties represent one standard deviation calculated by simple error propagation.

As shown in the Table 3, the values of m indicate that MIP2 shows a much larger heterogeneity than MIP1 and MIP3. It is also interesting to notice that the number of sites ($N_{K_{min}-K_{max}}$) estimated for the MIP2 is twice to that of MIP1 and almost six times the calculated for MIP3. In all cases, the NIPs showed considerably smaller $N_{K_{min}-K_{max}}$ than the


© 2012 WILEY-VCH Verlag GmbH & Co. KGaA, Weinheim

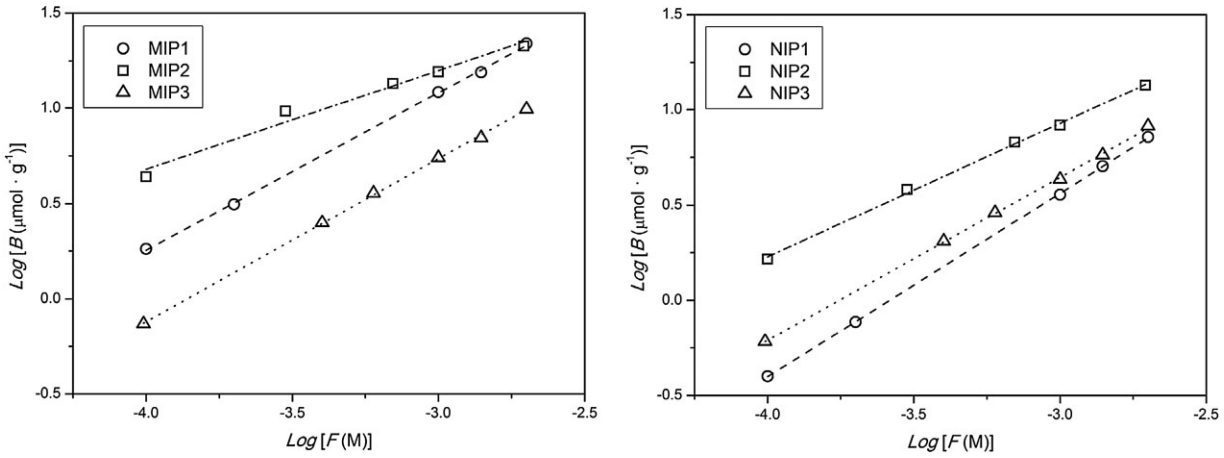


*Figure 5.* Experimental binding isotherm obtained for (**1**) in the series of polymers studied and their corresponding fits to Equation 2. Fitting of the isotherms provided $R^2 > 0.96$ in all cases.

*Table 3.* Experimental *a*, *m*, weighted average affinity ($\overline{K}_{K_{min}-K_{max}}$) and the number of sites ($N_{K_{min}-K_{max}}$) calculated for the series of MIPs studied. Calculations are for the range $K_{min} = 500\ M^{-1}$, $K_{max} = 10\,000\ L \cdot molmol^{-1}$.

| Polymer | *a* [(μmol · g$^{-1}$) (L · mol$^{-1}$)$^m$] | *m* | $N_{K_{min}-K_{max}}$ [μmol · g$^{-1}$] | $\overline{K}_{K_{min}-K_{max}}$ [L · mol$^{-1}$] |
|---|---|---|---|---|
| MIP1 | 3 600 ± 400 | 0.83 ± 0.01 | 6.5 ± 0.8 | 1 800 ± 80 |
| NIP1 | 2 800 ± 400 | 0.96 ± 0.01 | 0.5 ± 0.1 | 1 600 ± 80 |
| MIP2 | 570 ± 90 | 0.52 ± 0.04 | 13 ± 3 | 2 000 ± 300 |
| NIP2 | 1 100 ± 200 | 0.70 ± 0.01 | 8 ± 1 | 1 900 ± 100 |
| MIP3 | 1 900 ± 300 | 0.85 ± 0.01 | 2.5 ± 0.3 | 1 800 ± 100 |
| NIP3 | 1 600 ± 200 | 0.85 ± 0.01 | 2.0 ± 0.3 | 1 800 ± 80 |

corresponding MIPs. Concerning the values of $\overline{K}_{K_{min}-K_{max}}$, within experimental uncertainties, all polymers show similar (average) affinities. The connotations of these observations are discussed at the end of this section. A polymer similar to MIP3 was previously studied by Urraca et al.[26] and the values of N and $\overline{K}$ reported were slightly larger than those obtained in this work. In principle, this difference can be attributed to the fact that Urraca et al.[26] used trimethyl trimethacrylate (TRIM) as crosslinker (instead of EGDMA) and to the temperature of synthesis of the polymers; while Urraca et al.[26] performed the syntheses at 4 °C, all polymers reported in this study were synthesized at room temperature (≈25 °C).

### 3.4. Nitrogen Sorption

The sorption isotherm for MIP2 is shown in Figure 6. The observed isotherm can be easily identified as a Type IV isotherm with type H3 and H4 hysteresis. This isotherm is consistent with that expected for a mesoporous material.[36] The nonclosure of the loop implies incomplete removal of the adsorbate from the narrowest pores. The BET and BJH surface areas, pore volumes and average pore diameters estimated for the polymer studied are collected in Table 4. Given the similarity of the experimental areas

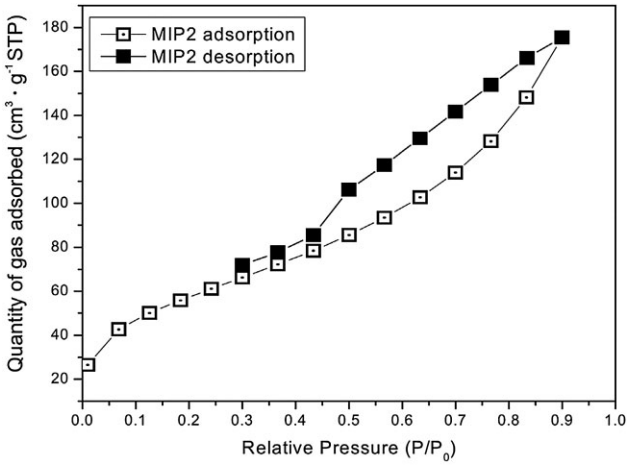


*Figure 6.* Sorption and desorption isotherms for the MIP2.


© 2012 WILEY-VCH Verlag GmbH & Co. KGaA, Weinheim

*Table 4.* Summary of the surface area and the pore data obtained for MIP of different morphologies and particle sizes.

| Polymer | BET surface area $A_{BET}$ [$m^2 \cdot g^{-1}$] | Cumulative volume of pores $V_{P,BJH}$ [$cm^3 \cdot g^{-1}$] | Average pore diameter $D_{P,BJH}$ [Å] |
|---|---|---|---|
| MIP1 | 221 | 0.19 | 41.5 |
| MIP2 | 207 | 0.19 | 42.2 |
| MIP3 | 231 | 0.17 | 42.2 |

and pore volumes reported in Table 4, it may be concluded that (**1**) should have comparable access to the surface and core of all particles, independently of their sizes and morphologies.

The analysis of the data in Table 3 can easily explain the chromatographic behavior of the polymers in the elution experiments, as well as to conclude on the molecular recognition capability of MIPs. The relationship between *m*, *N*, and $\overline{K}$ and the chromatographic performances of MIPs/NIPs has been firmly established in several fundamental contributions to the MIPs technology.[33,41,42,44,45] Generally, MIPs show larger heterogeneities of binding sites than the corresponding NIPs. NIPs are characterized by relatively higher m and lower values of *N* and $\overline{K}$; in other words, these polymers have comparatively few (and structurally similar) binding sites, most of them of low affinity. In contrast, numerous binding sites may be present in a MIP matrix, some of them of high affinity (larger *N* and $\overline{K}$). However, during the polymerization process, molecular recognition sites are created randomly and consequently, the structure and affinity of these biding sites differ markedly. This leads to a broader distribution of binding sites affinities and necessarily, to smaller *m*. Hence, as HPLC stationary phases, NIPs generally behave as materials of low capacity (*k*) and provide good shaped chromatograms; while the greater heterogeneity of MIPs leads to larger capacities but also, to broader and usually nonsymmetrical chromatographic peaks. As shown in Figure 3, this is the behavior observed for the MIPs/NIPs synthesized in this study. Additionally, considering that the calculated weighted average affinity ($\overline{K}$) are similar for all the polymers studied, it seems apparent that the main difference between these materials as stationary phases resides in the number of (specific and unspecific) binding sites (*N*). Note that there is a reasonable correlation between the calculated *N* and the retention factors (*k*) reported in Table 2; i.e., the larger the *N*, the larger the retention factor (or retention times). Comparing the values of *N* calculated for the corresponding MIP/NIP, conclusions about the capability for molecular recognition of MIPs can also be reached. This recognition capability should depend on $\Delta N = N_{MIP} - N_{NIP}$, since this difference represents approximately the number of specific binding sites in the MIP. The calculated $\Delta N$ are ≈6 (MIP1), ≈5 (MIP2), and ≈0.5 $\mu mol \cdot g^{-1}$ (MIP3). The value of $\Delta N$ for MIP3 synthesized (at 4 °C) by Urraca et al.[26] is ≈3 $\mu mol \cdot g^{-1}$. Hence, the proposed synthetic method does not only allow improving the morphology of the particles but also bring some advantages in terms of imprinting efficiency. However, a more appropriate comparison would be to contrast the rebinding capacities of the microbeads with that of a bulk polymer synthesized with toluene as porogen. It is known that toluene and acetonitrile behave differently as porogen. Although, there are general criteria that allows predicting (at least roughly) some of final characteristics of the polymers obtained using different type of porogens, the properties of MIPs synthesized (particularly, their capacity for molecular recognition, pore sizes, etc.) cannot be anticipated and need to be determined experimentally. For that reason, polymers MIP4 and NIP4 were synthesized. As mentioned in the Experimental Section, MIP4 and NIP4 do not meet the necessary mechanical properties for being used as HPLC stationary phases. Therefore, the comparison between the porogens could not be performed.

In order to better understand the nature of template/polymer interactions several experiments varying the mobile phase composition were conducted. It was noticed that the use of acetonitrile/water 90:10 vol% as mobile phase caused large decreases of the experimental retention times (and capacity factors) for all the polymers studied. Coincidentally, when the mobile phase used was (neat) methanol the eventual vanishing of the imprinting effect was observed. The large interference produced by the protic solvents suggests that both the specific and nonspecific interactions established between (**1**) and the polymers are mainly of the H-bonding type. This could explain the similar values of the calculated $\overline{K}$. What are somewhat harder to rationalize are the values of the estimated N for different polymers, in particular the relatively large values calculated for MIP2 and NIP2. However, it would not be surprising the small amounts of PVA on the surface of the microparticles could be responsible for the larger number of nonspecific interactions observed in these cases. It is worth remembering that in the particular case of MIP2, the IR studies did not allow concluding about the complete elimination of PVA.

To this regard, it would be very interesting to compare the chromatographic performance of microbeads prepared in the absence and in the presence of PVA, since such study could provide significant information about the disturbing role exerted by the stabilizer (PVA). However, this particular experiment cannot be carried-out because the SP technique (in all its variants, i.e., conventional and mini-SP, modified-SP) always requires the presence of PVA for stabilizing the prepolymeric suspension.


© 2012 WILEY-VCH Verlag GmbH & Co. KGaA, Weinheim

Finally, the fact that the microspheres showed acceptable molecular recognition capabilities seems to contradict previous assumptions indicating that the particles synthesized by the MSP technique should show poor performances to this regard.[17,18] The main reason for this assumption was based in the large (molar) excess of dispersing (water) and stabilizers (PVA, SDS) agents (relative to the functional monomer) required for the synthesis of the particles. In principle, these agents should compete with the functional monomer (2-DAEM) for the template disfavoring the imprinting efficiency. However, this seems not to be the case for the polymers studied herein. (**1**) is a highly hydrophobic compound and it should be preferentially residing in the (toluene) oily core of the prepolymeric microdroplets. This should be particularly true since the functional monomer (2-DAEM) and the cross-linker (EGDMA), both in large excess and capable of forming H-bonds, should be competing favorably with (**1**) for the –OH present at the microdroplet interface. Since the 2-DAEM molecules associated with the interface do not participate in the imprinting process, they may generate some superficial nonspecific binding sites after polymerization. However, note that even in the worse case; i.e., NIP2, the number of nonspecific sites ($N$) is only about 8 $\mu mol \cdot g^{-1}$, amount that is insignificant when compared with the moles of 2-DAEM used for the synthesis, this is: $\approx$800 $\mu mol \cdot g^{-1}$ of polymer. Hence, inside the microdroplets, the concentrations of 2-DAEM must be nearly the same than that of the synthesis in bulk, fact that explains why important changes in the recognition capability of the microbeads are not observed.

## 4. Conclusion

A comparative analysis of the affinity binding site's distribution of the MIPs and corresponding NIPs, showed that the microparticles synthesized using the modified SP technique (MIP1 and MIP2) have acceptable recognition capabilities. The modified SP technique is largely advantageous in terms of time-consuming and high yields of usable material and it should be considered as a viable alternative for the synthesis of imprinted HPLC stationary phases.

Acknowledgements: The authors thank the Consejo Nacional de Investigaciones Científicas y Técnicas (CONICET-Argentina), Agencia Nacional de Promoción Científica (FONCYT-Argentina), and Secretaría de Ciencia y Técnica (UNRC) for financial support. J. J. T. thanks CONICET-ACyT (Córdoba) for his PhD scholarship.

Received: July 15, 2011; Published online: November 3, 2011; DOI: 10.1002/mame.201100237

Keywords: affinity binding site distribution; heterogeneous polymers; high-performance liquid chromatography (HPLC); minisuspension polymerization; molecular imprinting

[1] a) M. Yan, O. Ramström, *Molecularly Imprinted Materials. Science and Technology*, Marcel Dekker, New York **2005**; b) M. Komiyama, T. Takeuchi, R. Mukawa, H. Asanuma, *Molecular Imprinting*, Wiley-VCH, Weinheim **2003**.
[2] T. A. Sergeyeva, O. A. Slinchenko, L. A. Gorbach, V. F. Matyushov, O. O. Brovko, S. A. Piletsky, L. M. Sergeeva, G. V. Elska, *Anal. Chim. Acta* **2010**, *659*, 274.
[3] M. Erdem, R. Say, A. Ersöz, A. Denizli, H. Türk, *Appl. Clay Sci.* **2010**, *47*, 223.
[4] G. Cirillo, M. Curcio, O. I. Parisi, F. Puoci, F. Iemma, U. G. Spizzirri, *Food Chem.* **2011**, *125*, 1058.
[5] Y. Li, X. Li, J. Chu, C. Dong, J. Qi, Y. Yuan, *Environ. Pollut.* **2010**, *158*, 2317.
[6] S. J. Ahmadi, O. Noori-Kalkhoran, S. Shirvani-Arani, *J. Hazard. Mater.* **2010**, *175*, 193.
[7] K. Mosbach, O. Ramström, *Nat. Biotechnol.* **1996**, *14*, 163.
[8] G. Wulff, *Angew. Chem., Int. Ed. Engl.* **1995**, *47*, 1812.
[9] L. Ye, P. A. G. Cormack, K. Mosbach, *Anal. Commun.* **1999**, *36*, 35.
[10] D. Vaihinger, K. Landfester, I. Kräuter, H. Brunner, G. E. M. Tovar, *Macromol. Chem. Phys.* **2002**, *203*, 1965.
[11] H. Sambe, K. Hoshina, J. Haginaka, *Anal. Sci.* **2005**, *21*, 391.
[12] N. Pérez-Moral, A. G. Mayes, *Anal. Chim. Acta* **2004**, *504*, 15.
[13] H. Khan, J. K. Park, *Biotechnol. Bioprocess Eng.* **2006**, *11*, 503.
[14] M. Andaç, R. Say, A. Denizli, *J. Chromatogr. B* **2004**, *811*, 119.
[15] X. Pang, G. Cheng, R. Li, S. Lu, Y. Zhang, *Anal. Chim. Acta* **2005**, *550*, 13.
[16] L. Zhang, G. Cheng, C. Fu, *React. Funct. Polym.* **2003**, *56*, 167.
[17] A. G. Mayes, K. Mosbach, *Anal. Chem.* **1996**, *68*, 3774.
[18] H. Kempe, M. Kempe, *Anal. Chem.* **2006**, *78*, 3659.
[19] J. C. Ramirez, J. Herrera-Ordones, *Eur. Polym. J.* **2007**, *43*, 3819.
[20] J. C. Ramirez, J. Herrera-Ordonez, V. A. Gonzalez, *Polymer* **2006**, *47*, 3336.
[21] J. Philip, G. Gnanaprakash, T. Jayakumar, P. Kalyanasundaram, B. Raj, *Macromolecules* **2003**, *36*, 9230.
[22] H. Khan, T. Khan, J. K. Park, *Sep. Purif. Technol.* **2008**, *62*, 363.
[23] X. B. Wang, Z. H. Zheng, X. B. Ding, X. Cheng, X. H. Hu, Y. X. Peng, *Chin. Chem. Lett.* **2006**, *17*, 1243.
[24] A. G. Strikovsky, D. Kasper, M. Grün, B. S. Green, J. Hradil, G. Wulff, *J. Am. Chem. Soc.* **2000**, *122*, 6295.
[25] K. Hosoya, K. Yoshizako, N. Tanaka, K. Kimata, T. Araki, J. Haginaka, *Chem. Lett.* **1994**, 1437.
[26] J. L. Urraca, M. D. Marazuela, E. R. Merino, G. Orellana, M. C. Moreno-Bondi, *J. Chromatogr. A* **2006**, *1116*, 127.
[27] R. L. Bates, P. L. Fondy, R. R. Corpstein, *Ind. Eng. Chem. Process Des. Dev.* **1963**, *2*, 310.
[28] A. W. Nienow, D. Miles, *Ind. Eng. Chem. Process. Des. Dev.* **1971**, *10*, 41.
[29] J. Oxelbark, C. Legido-Quigley, C. Aureliano, M. Titirici, E. Schillinger, B. Sellergren, J. Courtois, K. Irgum, L. Dambies, P. Cormack, D. Sherrington, E. De Lorenzi, *J. Chromatogr., A* **2007**, *1160*, 215.
[30] J. J. Kirkland, J. J. DeStefano, *J. Chromatogr. A* **2006**, *1126*, 50.
[31] J. A. García-Calzón, M. E. Díaz-García, *Sens. Actuators B* **2007**, *123*, 1180.
[32] P. P. Ylä-Mäihäniemi, D. R. Williams, *Langmuir* **2007**, *23*, 4095.
[33] A. M. Rampey, R. J. Umpleby, II, G. T. Rushton, J. C. Iseman, R. N. Shah, K. D. Shimizu, *Anal. Chem.* **2004**, *76*, 1123.


© 2012 WILEY-VCH Verlag GmbH & Co. KGaA, Weinheim

[34] E. P. Barrett, L. Joyner, P. P. Halenda, *J. Am. Chem. Soc.* **1951**, *73*, 373.
[35] D. M. Ruthven, *Principles of Adsorption and Adsorption Processes*, New York John Wiley & Sons, **1984**.
[36] K. S. W. Sing, *Pure Appl. Chem.* **1982**, *52*, 2201.
[37] N. Holland, J. Frisby, E. Owens, H. Hughes, P. Duggan, P. McLoughlin, *Polymer* **2010**, *51*, 1578 and reference therein.
[38] F. Bai, X. Yang, W. Huang, *Eur. Polym. J.* **2006**, *42*, 2088.
[39] H. S. Mansur, C. M. Sadahira, A. N. Souza, A. A. P. Mansur, *Mater. Sci. Eng., C* **2008**, *28*, 539.
[40] H. Kim, K. Kaczmarski, G. Guiochon, *Chem. Eng. Sci.* **2005**, *60*, 5425.
[41] P. Sajonza, M. Kelea, G. Zhonga, B. Sellergren, G. Guiochon, *J. Chromatogr., A* **1998**, *810*, 1.
[42] B. Tóth, T. Pap, V. Horvath, G. Horvai, *J. Chromatogr. A* **2006**, *1119*, 29.
[43] B. Tóth, K. László, G. Horvai, *J. Chromatogr. A* **2005**, *1100*, 60.
[44] R. J. Umpleby, II, S. C. Baxter, A. M. Rampey, G. T. Rushton, Y. Chen, K. D. Shimizu, *J. Chromatogr. B* **2004**, *804*, 141.
[45] R. J. Umpleby, II, S. Baxter, M. Bodea, J. Berch, Jr., R. Shaha, K. D. Shimizu, *Anal. Chim. Acta* **2001**, *435*, 35.


© 2012 WILEY-VCH Verlag GmbH & Co. KGaA, Weinheim